Involvement of Free Nitrenium Ions, Ion Pairs, and Preassociation Trapping in the Reactions of Ester Derivatives of *N*-Arylhydroxylamines and *N*-Arylhydroxamic Acids in Aqueous Solution

Michael Novak,* Mary Jo Kahley, Jing Lin, Sonya A. Kennedy, and Tishia G. James

Department of Chemistry, Miami University, Oxford, Ohio 45056

Received May 19, 1995[⊗]

Rate and product yield data for the decomposition of the ester derivatives of *N*-arylhydroxylamines and *N*-arylhydroxamic acids **1a–i** in aqueous solution in the presence of N_3^- support a mechanistic scheme (Scheme 5) in which the trapping by N_3^- changes from trapping of the free ion, to trapping of an ion pair, to a preassociation process as the ion becomes more reactive. When the rate constant for trapping of the free ion by solvent, k_s, $< \sim 10^8$ s^{-1}, trapping by both N_3^- and solvent occurs almost exclusively at the free ion. When 10^8 s$^{-1} < \sim k_s < \sim 10^{10}$ s^{-1}, a change in the mechanism occurs, and trapping of the ion pair by both solvent and N_3^- becomes important. In this range of reactivity there is also evidence, based on the apparent magnitude of k_{az}', the rate constant for N_3^- trapping of the ion pair, that some of the reaction with N_3^- occurs though a preassociation process. When $k_s > \sim 10^{10}$ s^{-1} essentially all of the observed N_3^- trapping occurs by a preassociation process because N_3^-, which cannot react with the ion pair faster than the diffusion limit, can no longer compete with solvent for the ion pair. This progression in trapping mechanisms as the ion becomes more reactive with solvent is apparently an important factor in determining the carcinogenic potential of aromatic amines and amides which are metabolized into sulfuric and carboxylic acid esters of *N*-arylhydroxylamines and *N*-arylhydroxamic acids. Nitrenium ions that undergo slow reactions with solvent are selectively trapped by biologically relevant nucleophiles such as 2′-deoxyguanosine. As the rate constant for reaction with solvent increases, the nitrenium ion is no longer capable of undergoing selective trapping by nonsolvent nucleophiles because these reactions are rate limited by diffusion, but solvent trapping is not.

Carboxylic or sulfuric acid esters of *N*-arylhydroxylamines and *N*-arylhydroxamic acids **1** have been implicated as the ultimate carcinogens derived from metabolic activation of aromatic amines and amides.[1] It is now well established that a number of esters of this type generate reactive nitrenium ions **3** by rate-limiting N–O bond cleavage during their hydrolysis reactions.[2] We have recently shown that the *N*-acetyl-*N*-(4-biphenylyl)- and *N*-acetyl-*N*-(2-fluorenyl)nitrenium ions, **3h** and **3i**, are efficiently trapped by 2′-deoxyguanosine in aqueous solution so these ions could be responsible for the carcinogenic effects of the parent esters.[3]

Since the addition of nucleophiles to the hydrolysis reaction mixtures does not have a significant effect on the yield of the rearrangement products **8** or **9** in the cases which we have reported previously, we have generally concluded that the ion pair, **2**, is not effectively trapped by these nucleophiles, and we have explained the trapping behavior in terms of the mechanism of Scheme 1.[2] This is an adequate description of the behavior of the less reactive and more selective ions such as **3h** and **3i**, but as the ions become more reactive the ion pair **2** must begin to play a role in the hydrolysis chemistry of **1** because the ion will be trapped by solvent or other nucleophiles before the leaving group can diffuse away.[4] In extreme cases a preassociation mechanism may also become important.[4,5]

Fishbein and McClelland have recently provided experimental evidence for the existence of a number of short-lived ion pairs which must be invoked to explain the hydrolysis behavior of *O*-aroyl-*N*-acetyl-N-(2,6-dimethylphenyl)hydroxylamines **10**.[6] Since these studies

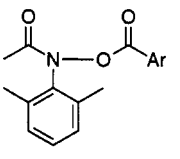

10

were done with a single nitrenium ion component of the ion pair, it was not possible to examine the effect of nitrenium ion stability on the hydrolysis mechanism. The effect that aryl substituents and the second N-substituent have on the involvement of ion pairs in the hydrolysis of the esters **1a–i** (X = SO_3^- or C(O)-*t*-Bu) is examined herein. A progression in the mechanism of trapping by

[⊗] Abstract published in *Advance ACS Abstracts,* September 1, 1995.

(1) Miller, J. A. *Cancer Res.* **1970**, *30*, 559–576. Kriek, E. *Biochem. Biophys. Acta* **1974**, *335*, 177–203. Miller, E. C. *Cancer Res.* **1978**, *38*, 1479–1496. Miller, E. C.; Miller J. A. *Cancer* **1981**, *47*, 2327–2345. Miller, J. A.; Miller, E. C. *Environ. Health Perspect.* **1983**, *49*, 3–12. Garner, R. C.; Martin, C. N.; Clayson, D. B. In *Chemical Carcinogens*, 2nd ed.; Searle, C. E., Ed.; ACS Monograph 182; American Chemical Society: Washington, DC, 1984; Vol. 1, pp 175–276. Beland, F. A.; Kadlubar, F. F. *Environ. Health Perspect.* **1985**, *62*, 19–30. Kadlubar, F. F.; Beland, F. A. In *Polycyclic Hydrocarbons and Carcinogenesis;* ACS Symposium Series 283; American Chemical Society: Washington, DC, 1985; pp 341–370.

(2) (a) Novak, M.; Kahley, M. J.; Eiger, E.; Helmick, J. S.; Peters, H. E. *J. Am. Chem. Soc.* **1993**, *115*, 9453–9460. (b) Novak, M.; Kahley, M. J.; Lin, J.; Kennedy, S. A.; Swanegan, L. A. *J. Am. Chem. Soc.* **1994**, *116*, 11626–11627.

(3) Novak, M.; Kennedy, S. A. *J. Am. Chem. Soc.* **1995**, *117*, 574–575.

(4) Richard, J. P.; Jencks, W. P. *J. Am. Chem. Soc.* **1984**, *106*, 1373–1383. Richard, J. P.; Amyes, T. L.; Vontor, T. *J. Am. Chem. Soc.* **1991**, *113*, 5871–5873.

(5) Jencks, W. P. *Chem. Soc. Rev.* **1981**, *10*, 345–375.

(6) Fishbein, J. C.; McClelland, R. A. *J. Chem. Soc., Perkin Trans. 2* **1995**, 663–671.

0022-3263/95/1960-8294$09.00/0

Scheme 1

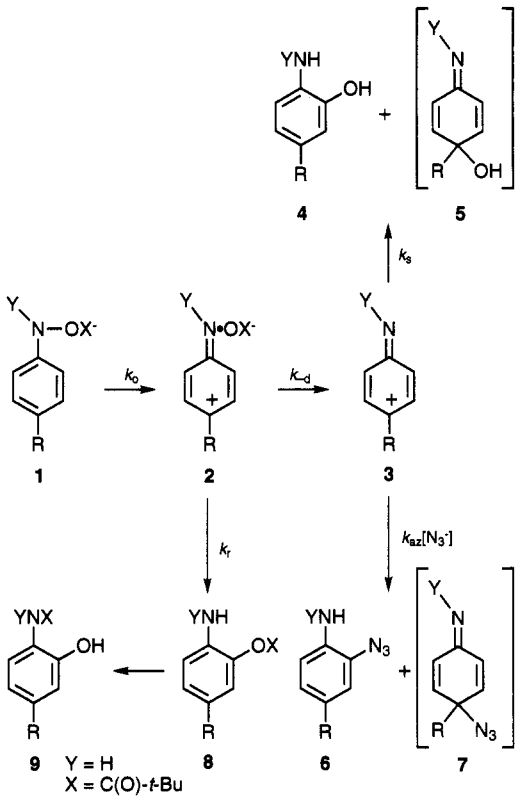

	R	Y	X
a	H	Ac	SO_3^-
b	CH_3	H	C(O)-*t*-Bu
c	CH_3	Ac	SO_3^-
d	Cl	H	C(O)-*t*-Bu
e	Cl	Ac	SO_3^-
f	OEt	Ac	C(O)-*t*-Bu
g	Ph	H	C(O)-*t*-Bu
h	Ph	Ac	SO_3^-
i	RPh = 2-fluorenyl	Ac	SO_3^-

N_3^- from trapping of the free ion, to trapping of the ion pair, to a preassociation process is observed as the ion becomes more reactive.

Results and Discussion

Rate constants and product yields for the hydrolysis of seven potential nitrenium ion precursors (**1a–f,i**) in 5% CH_3CN-H_2O (μ = 0.5 ($NaClO_4$)), T = 20 °C (**1b–d,f,i**) or 50 °C (**1a,e**) in the presence or absence of N_3^- are presented in the supporting information. In all reactions constant pH was maintained with N_3^-/HN_3 buffers or with low concentration (0.001–0.02 M) NaOAc/HOAc or Na_2HPO_4/NaH_2PO_4 buffers. Rate and product data for the hydrolysis of **1g** and **1h** under the same conditions at 20 °C were reported previously.[2a] In all cases hydrolysis rate constants are essentially independent of $[N_3^-]$. The largest change observed was a ca. 15% increase in k_{obs} for **1d** as $[N_3^-]$ was increased from 0 to 0.475 M. This rate increase is not correlated with azide adduct yield which reaches 72% at 0.475 M N_3^-. The small rate constant increase observed in this case is consistent with a specific salt effect, not a kinetically bimolecular reaction of **1d** with N_3^-. The lack of rate dependence on $[N_3^-]$ is

Scheme 2

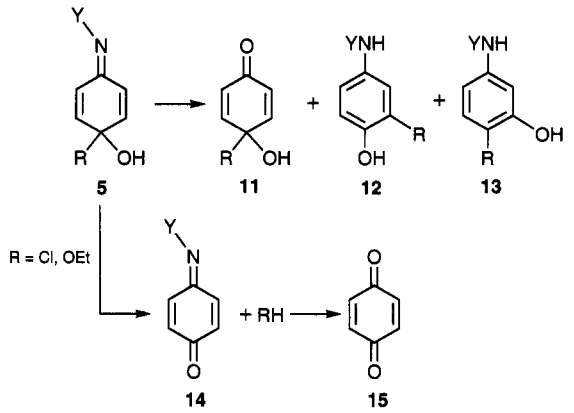

consistent with a mechanism involving rate-limiting ionization ($k_{obs} = k_o$ of Scheme 1), but this observation does not rule out preassociation mechanisms in which N_3^- provides no significant assistance to ionization.[4,5]

The stable hydrolysis products obtained in the absence of N_3^- consisted of **4**, **11–13**, and **15** (Schemes 1 and 2). The products obtained in individual cases were highly dependent on the aromatic substituent R and the N-substituent Y. We have previously shown that the products **11–13** and **15** are obtained from subsequent reactions of the initial unstable hydrolysis product **5** that has been observed as a transient species in a number of cases[2,7] or from the quinone imine **14** that is apparently derived from **5** and has also been detected if R = O–alkyl (Scheme 2).[8] The mechanisms for the formation of these products from **5** have been discussed previously[2,7–9] and will not be considered here.

In the presence of N_3^- all of the esters yield **6** and in several cases (**1a,d–f**) products (**17**, **20**, and **21**) which appear to be derived from an unstable initial adduct **7** (Scheme 3). The adduct **7** has not been detected, but evidence presented below indicates that it is an initial reaction product in a number of cases.

We have shown previously that the yields of solvent- and N_3^--derived products vary with $[N_3^-]$ in a manner apparently consistent with competitive N_3^- and solvent attack on a common species.[2] Since hydrolysis rate constants are independent of $[N_3^-]$ we concluded that N_3^- and solvent compete for a nitrenium ion intermediate, at least for the less reactive ions, and we have interpreted our results in terms of Scheme 1.[2] The experimentally observed N_3^-/solvent selectivity ratio, S, determined from the product yield data[10] is equivalent to k_{az}/k_s of Scheme 1 if the mechanism of that scheme describes the reaction process. Directly measured k_{az} and k_s for **3g–i** generated by laser flash photolysis are consistent with k_{az}/k_s ratios estimated for these ions from product data.[2,11] These

(7) Novak, M.; Roy, A. K. *J. Org. Chem.* **1985**, *50*, 571–580. Panda, M.; Novak, M.; Magonski, J. *J. Am. Chem. Soc.* **1989**, *111*, 4524–4525. Novak, M.; Helmick, J. S.; Oberlies, N.; Rangappa, K. S.; Clark, W. M.; Swenton, J. S. *J. Org. Chem.* **1993**, *58*, 867–878.

(8) Novak, M.; Pelecanou, M.; Pollack, L. *J. Am. Chem. Soc.* **1986**, *108*, 112–120. Novak, M.; Pelecanou, M.; Zemis, J. N. *J. Med. Chem.* **1986**, *29*, 1424–1429.

(9) Gassman, P. G.; Granrud, J. E. *J. Am. Chem. Soc.* **1984**, *106*, 2448–2449. Biggs, T. N.; Swenton, J. S. *J. Am. Chem. Soc.* **1993**, *115*, 10416–10417.

(10) S = $[N_3^-$-adducts]/([solvent-adducts]·$[N_3^-]$). This ratio is constant and formally equivalent to k_{az}/k_s if N_3^- and solvent compete for the same intermediate as in Scheme 1.

(11) Davidse, P. A.; Kahley, M. J.; McClelland, R. A.; Novak, M. *J. Am. Chem. Soc.* **1994**, *116*, 4513–4514. McClelland, R. A.; Davidse, P. A.; Hadzialic, G. *J. Am. Chem. Soc.* **1995**, *117*, 4173–4174.

Scheme 3

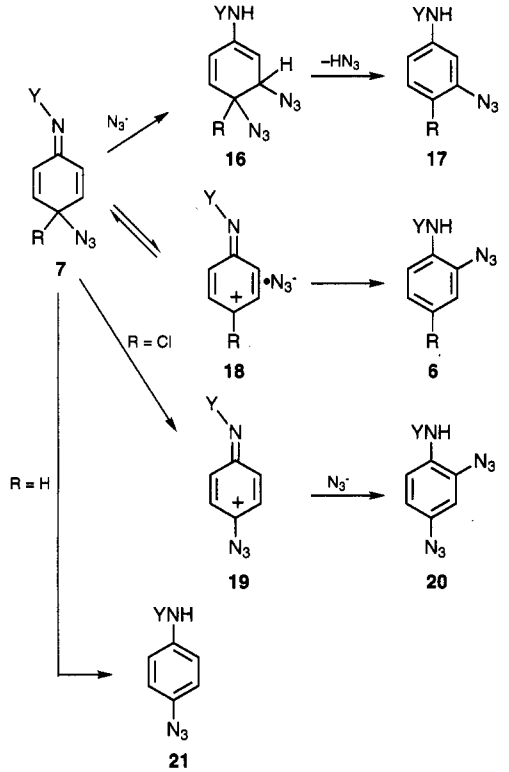

Scheme 4

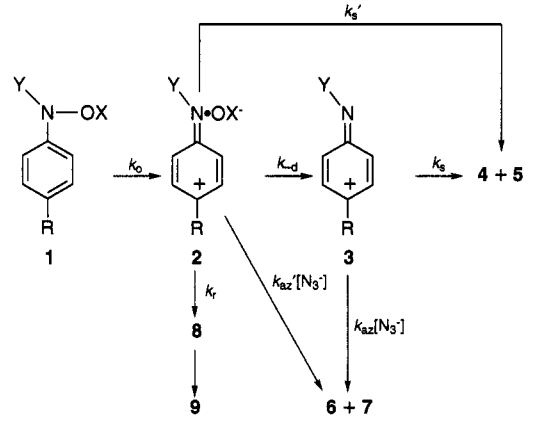

data also confirmed the assumption that k_{az} is diffusion limited at ca. 5×10^9 M^{-1} s^{-1} for these three ions.[2,11,12]

The mechanism of Scheme 1 is an over-simplification since it does not consider the possibility of trapping of the ion pair **2** by solvent or N_3^-. When the magnitude of the rate constant for trapping of **2** by solvent (k_s' of Scheme 4) approaches that of k_{-d}, trapping of the ion pair will become important.[4] If $k_s \approx k_s'$ and k_{az} (and k_{az}') is diffusion limited at ca. 5×10^9 M^{-1} s^{-1}, k_{az}/k_s, or the experimentally observed selectivity ratio, S, will indicate whether reaction at the ion pair becomes important. When k_s' becomes so large that diffusional processes cannot compete with it, any reaction with nonsolvent nucleophiles, such as N_3^-, must occur by a preassociation mechanism (Scheme 5).[4,5] The examples discussed below show the progression from trapping of the free ion, to trapping of the ion pair, to a preassociation process.

(12) For **3i** the directly measured k_{az} is slightly below the apparent diffusion limit at 4.2×10^9 M^{-1} s^{-1} (ref 11). This may indicate the onset of an activation-controlled reaction of N_3^- with nitrenium ions more stable than **3i**.

Scheme 5

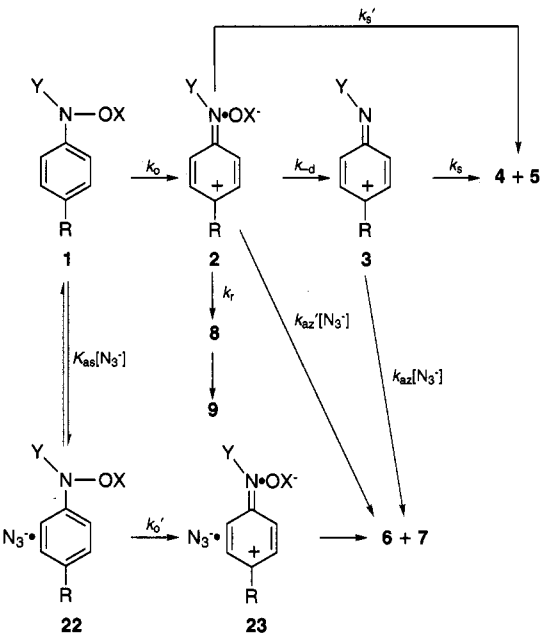

Since the selectivity ratio, S, characterizes this progression, that ratio is used to classify the examples shown below.

100 $M^{-1} \leq S \leq 6 \times 10^4$ M^{-1}. The ultimate carcinogen **1i** is a typical example of the compounds in this class. Added N_3^- traps the intermediate nitrenium ion to >99% at low [N_3^-] (ca. 1.7 mM for **1i**). The yield of the rearrangement product **8** or **9** is typically very low (ca. 2% for the combined yield of **8i** and **8i′** (eq 1)) and is

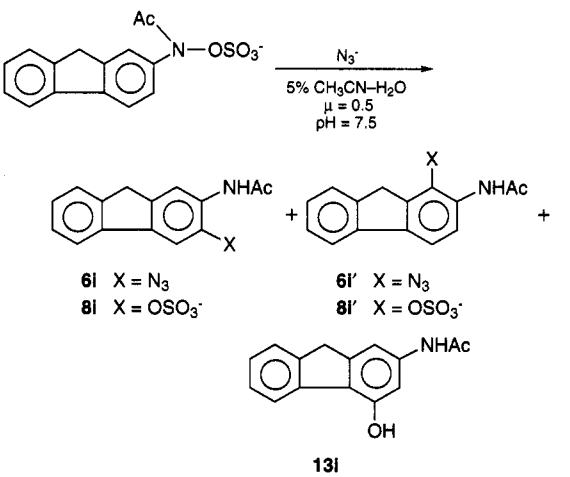

(1)

apparently unaffected by N_3^- at concentrations up to and including those necessary to trap the nitrenium ion to >99%. The mechanism of Scheme 1 is adequate to describe the kinetics and product study results quantitatively.

The % yields of N_3^-- and solvent-derived products and the rearrangement products are given by eqs 2, 3, and 4, respectively, if the mechanism of Scheme 1 is used to describe the data.

$$\%\ \text{azide prods} = \left(\frac{k_{-d}}{k_r + k_{-d}}\right)\left(\frac{k_{az}[N_3^-]}{k_s + k_{az}[N_3^-]}\right)100 \quad (2)$$

$$\%\ \text{solvent prods} = \left(\frac{k_{-d}}{k_r + k_{-d}}\right)\left(\frac{k_s}{k_s + k_{az}[N_3^-]}\right)100 \quad (3)$$

$$\% \text{ rearranged prods} = \frac{k_r}{k_r + k_{-d}}100 \qquad (4)$$

It has been determined that k_{az} is diffusion limited at ca. 5×10^9 M^{-1} s^{-1} for **3g–i**.[11] We have used that approximate value for k_{az} throughout this paper.[13] Diffusional separation of an anion–cation pair in aqueous solution appears to occur with a rate constant of ca. 10^{10}–10^{11} s^{-1}.[14] We have used a value of 10^{10} s^{-1} for k_{-d} in all of our fits.[15] For **1i** the product data as a function of $[N_3^-]$ are fit very well by eqs 2–4 with $k_r = 2 \times 10^8$ s^{-1} and $k_s = 8.1 \times 10^4$ s^{-1} (Figure 1). The ratio of the two isomeric azide adducts [**6i**]/[**6i'**] is constant at 2.5 ± 0.1 up to the highest $[N_3^-]$ examined (10.0 mM). This ratio and k_{az}/k_s are also unaffected by a change in the leaving group in **1i** from SO_4^{2-} to *t*-$BuCO_2^-$.[2b] All of these observations are consistent with the mechanism of Scheme 1.

The kinetic and product data for **1f–h** are also fit quantitatively by Scheme 1. Best-fit values for k_r, k_s, and k_{az}/k_s are listed in Table 1 for all four esters. Error limits on individual rate constants are approximately ±20% within the limits imposed by the assumptions concerning k_{-d} and k_{az}. The values of k_{az}/k_s reported here are essentially equivalent to the selectivity ratios, *S*, reported earlier from an alternative analysis of the product data.[2] Addition of terms for trapping of the ion pair **2** by solvent or N_3^-, as in Scheme 4, has no discernable effect on the fits because k_s' is too small to compete significantly with k_{-d} for these selective ions and k_{az}' $[N_3^-]$ will also not compete with k_{-d} at $[N_3^-]$ necessary to provide >95% trapping of **3** for all four esters ($[N_3^-] < 0.05$ M).

Hydrolysis of **1f** in the presence of N_3^- yields three azide adducts, **6f**, **17f**, and **24** (eq 5). The acetamidophenol **24** is not a product of N_3^- trapping of a nitrenium ion. Control experiments show that **24** is generated by N_3^- reaction with authentic **14**, Y = Ac, which is the exclusive initial solvent-derived product observed in the hydrolysis reaction of **1f**.[8] At the lowest $[N_3^-]$ employed (0.5 mM) ca. 60% of **14**, Y = Ac, is trapped by N_3^- to generate **24**. The remaining product is accounted for by the expected hydrolysis product[8] *p*-benzoquinone, **15**. In all the data analyses performed here **24** is considered as a product of solvent attack on the nitrenium ion **3f**. The relative yields of the two azide adducts which are derived from trapping of **3f** are not constant as $[N_3^-]$ is varied, although the sum of their yields is fit very well by the model of Scheme 1 (Figure 2A). These results can be explained if the intermediate **7f** is produced as an initial product, which subsequently decomposes into both **6f** and **17f** by the mechanism of Scheme 3. The data in Figure 2B were adequately fit if **6f** and **7f** are initially formed in a 1/10 ratio, and the N_3^--dependent ratio for partitioning of **7f** into **17f** and **6f** is 10 M^{-1}.[16] In this analysis it is assumed that the ion pair **18f** can lead only to **6f** or **7f**. This requires that the collapse of the ion pair **18f** to products occurs with a significantly larger rate constant than diffusional separation of the ion pair (ca. 10^{10} s^{-1}).

Products similar to **17f** were not found in the reaction mixtures of the other three esters. This may be due to an unusually high degree of formation of **7f** compared to **7g–i**, or to a partitioning ratio for **7g–i** which favors the ortho-substituted products **6g–i** at the low $[N_3^-]$ em-

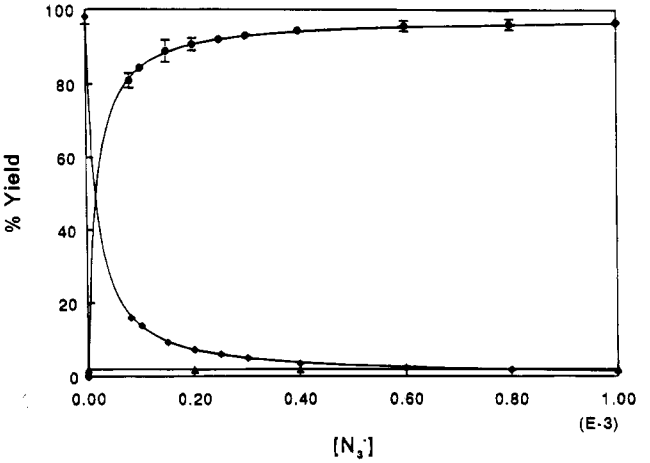

Figure 1. Product yields vs $[N_3^-]$ for **1i** at pH 7.4 in 0.001 M Na_2HPO_4/NaH_2PO_4 buffers: (●): **6i** and **6i'**, (♦) **13i**, (▲) **8i** and **8i'**. The theoretical curves were calculated from eqs 2–4 for the mechanism of Scheme 1 and the rate constants in Table 1.

Table 1. Best Fit Values of Rate Constants for the Mechanism of Scheme 1 for 1f, 1g, 1h, and 1i[a]

ester	k_r [b] (s^{-1})	k_s [c] (s^{-1})	k_{az}/k_s [d] (M^{-1})
1f	7×10^8	9.1×10^6	5.5×10^2
1g	5×10^8	1.5×10^6	3.3×10^3
1h	2×10^8	4.9×10^6	1.0×10^3
1i	2×10^8	8.1×10^4	6.2×10^4

[a] Conditions: 5% CH_3CN–H_2O, $\mu = 0.5$ ($NaClO_4$), $T = 20$ °C. [b] Average value required by eq 4 if $k_{-d} = 10^{10}$ s^{-1}. Estimated error limits in k_r ca. ±20%. [c] Determined from least-squares fit of the product data to eqs 2 and 3 with k_r determined as above, $k_{-d} = 10^{10}$ s^{-1} and $k_{az} = 5 \times 10^9$ M^{-1} s^{-1}. Estimated error limits in k_s ca. ±20%. [d] Assuming $k_{az} = 5 \times 10^9$ M^{-1} s^{-1}.

(13) Use of the directly measured k_{az} for **3g–i** would not materially change the conclusions made here. The approximate value of 5×10^9 M^{-1} s^{-1} was used for consistency in comparisons of the fits reported here.

(14) Hand, E. S.; Jencks, W. P. *J. Am. Chem. Soc.* **1975**, *97*, 6221–6230. Eigen, M. *Angew. Chem., Int. Ed. Engl.* **1964**, *3*, 1–19.

(15) An increase in the value of k_{-d} would require a proportional increase in k_r for the fits to Scheme 1, but k_{az}/k_s would be unchanged. For Schemes 4 and 5 an increase in k_{-d} would require approximately proportional increases in k_r and k_{az}' to maintain fits similar to those shown in Figures 3 and 4. The values of k_s' and k_{az}/k_s are significantly less strongly affected.

(16) The theoretical lines in Figure 2B are drawn from the following equations:

$$\mathbf{6f}\,(\%) = \left(\frac{k_{-d}}{k_r + k_{-d}}\right)\left(\frac{0.09k_{az}[N_3^-]}{k_s + k_{az}[N_3^-]} + \left(\frac{0.91\,k_{az}[N_3^-]}{k_s + k_{az}[N_3^-]}\right)\left(\frac{1}{1 + 10[N_3^-]}\right)\right)100$$

$$\mathbf{17f}\,(\%) = \left(\frac{k_{-d}}{k_r + k_{-d}}\right)\left(\frac{0.91k_{az}[N_3^-]}{k_s + k_{az}[N_3^-]}\right)\left(\frac{10[N_3^-]}{1 + 10[N_3^-]}\right)100$$

All rate constants are identical to those in Table 1.

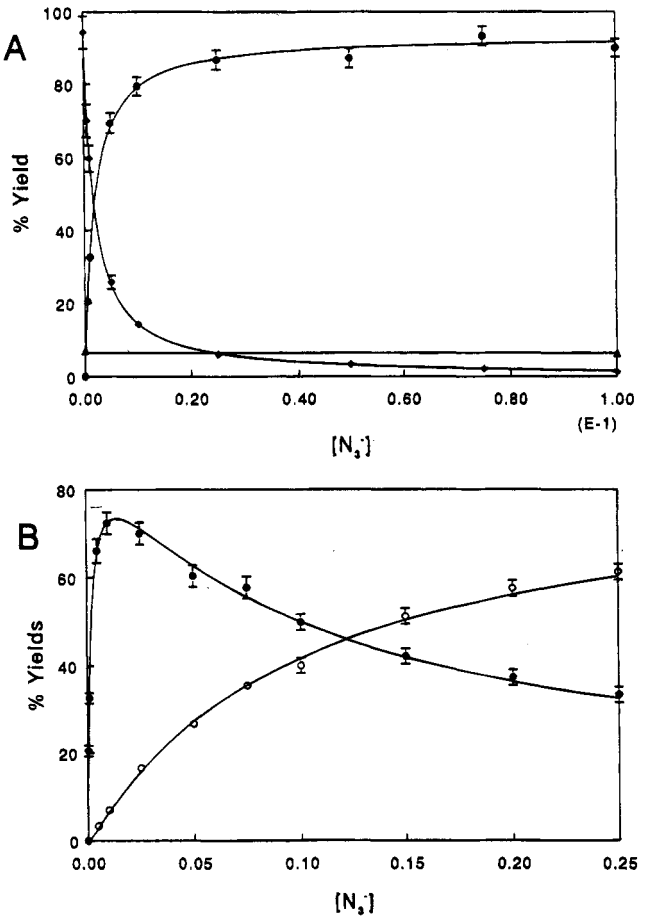

Figure 2. (A) Product yields vs $[N_3^-]$ for **1f** at pH 4.6 in 1/1 N_3^-/HN_3 buffers: (●) **6f** and **17f**, (♦) **15** if $[N_3^-] = 0$ M, **15** and **24** under all other conditions, (▲): **8f**. The theoretical curves were calculated from eqs 2–4 for the mechanism of Scheme 1 and the rate constants in Table 1. (B) Variation in the yields of **6f** and **17f** with $[N_3^-]$. The theoretical lines were calculated as described in the text.

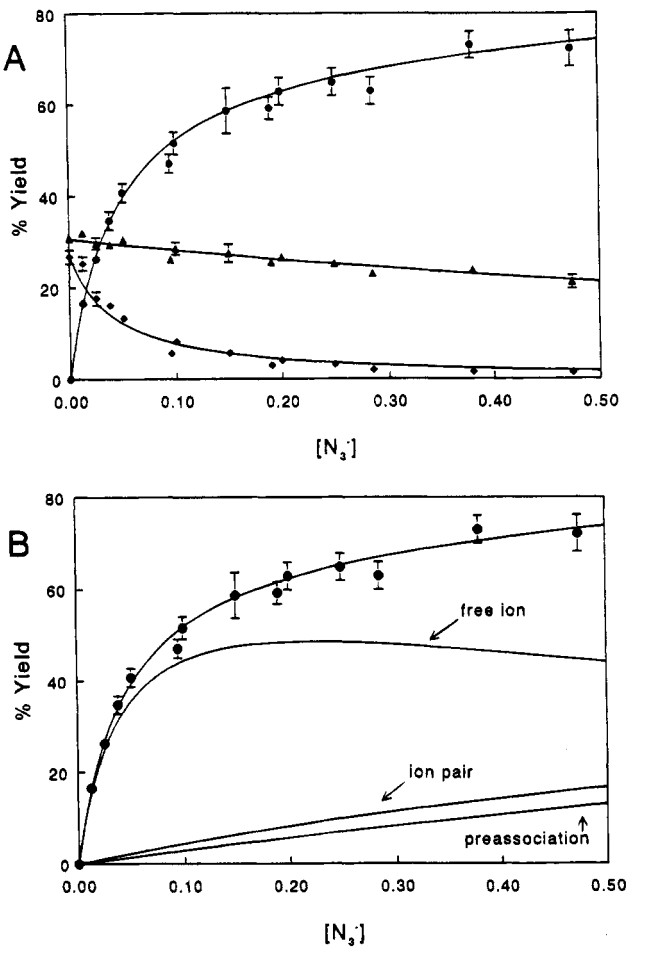

Figure 3. (A) Product yields vs $[N_3^-]$ for **1d** at pH 5.6 in 19/1 N_3^-/HN_3 buffers: (●) **6d** and **20**, Y = H, (♦) **4d**, (▲) **9d**. The theoretical curves were calculated from eqs 6–8 for the mechanism of Scheme 4 and the rate constants in Table 2. Nearly identical fits were obtained by fitting the data to eqs 11–13 for the mechanism of Scheme 5. (B) The fit of the N_3^- adduct product yields for **1d** vs $[N_3^-]$ to the preassociation mechanism of Scheme 5. The theoretical curve was calculated from eq 11 and the rate constants in Table 2. The contributions that the free ion, ion pair, and preassociation paths make to the overall N_3^- trapping are indicated.

ployed in these studies. The resonance donating OEt is likely to strongly localize the charge at the para-position of the aromatic ring in **3f** making attack at that position electrostatically favored.

$1\ M^{-1} \leq S \leq 100\ M^{-1}$. The product yield data as a function of $[N_3^-]$ for **1d** shown in Figure 3A are considerably different from those shown in Figures 1 and 2. The rearrangement product **9d** is a much larger part of the reaction mixture (32% at $[N_3^-] = 0$ M). As $[N_3^-]$ increases, the yield of this product decreases noticeably, falling by about 30% as $[N_3^-]$ increases from 0 to 0.5 M. The yield of the hydrolysis product **4d** falls off more rapidly with $[N_3^-]$, reaching about 50% of its initial yield at $[N_3^-] = 0.05$ M.[17] The combined yield of the two azide adducts **6d** and **20**, Y = H, has not reached a saturation limit at $[N_3^-] = 0.5$ M. Trapping by N_3^- is much less efficient than in the previous examples.

The product data cannot be fit by the mechanism of Scheme 1 because that mechanism cannot account for decreased yields of **9d** as $[N_3^-]$ increases. The mechanism of Scheme 4, which includes trapping by solvent and N_3^- of the ion pair, can quantitatively account for the product data. The product yields vary with $[N_3^-]$ according to eqs 6–8

$$\%\ \text{azide prods} = \left(\frac{1}{F}\right)\left(k_{az}'[N_3^-] + \frac{k_{-d}k_{az}[N_3^-]}{k_s + k_{az}[N_3^-]}\right)100 \quad (6)$$

$$\%\ \text{solvent prods} = \left(\frac{1}{F}\right)\left(k_s' + \frac{k_{-d}k_s}{k_s + k_{az}[N_3^-]}\right)100 \quad (7)$$

$$\%\ \text{rearranged} = \left(\frac{k_r}{F}\right)100 \quad (8)$$

where $F = k_r + k_{-d} + k_s' + k_{az}'[N_3^-]$. To fit the data we assumed $k_{-d} = 10^{10}\ s^{-1}$, $k_{az} = 5 \times 10^9\ M^{-1}\ s^{-1}$, and $k_s = k_s'$.[15] It is possible that the counterion of **2** can serve as a general base to accelerate the attack of H_2O, but our

(17) For **1d** the only solvent-derived product which could be analyzed for reliably was **4d**. The strongly absorbing N_3^-/HN_3 obscures the HPLC peaks of some products, and N_3^- traps authentic **14**, Y = H, to lead to a number of products which have not yet been identified (Novak, M.; James, T. G. Work in progress). For **1e**, **14**, Y = Ac, which is a major product of solvent attack on **2e** or **3e**,[20] is trapped by N_3^- to generate **24**. This product was identified but not quantified due to interference from the N_3^-/HN_3 HPLC peak at high $[N_3^-]$.

Table 2. Best Fit Values of Rate and Equilibrium Constants for Product Data Fit to the Mechanisms of Schemes 4 and 5[a]

ester	mechanistic scheme and temp (°C)	k_r [b] (s^{-1})	$k_s = k_s'$ [b] (s^{-1})	k_{az}' [b] ($M^{-1}\ s^{-1}$)	K_{as} [c] (M^{-1})	k_{az}/k_s [d] (M^{-1})
1a	5, 50	2.3×10^{11}	1.7×10^{11}[e]	5×10^{9}[f]	0.25	0.03
1b	5, 20	1.7×10^{9}	1.3×10^{9}	5×10^{9}	0.3	3.8
1c	5, 20	3.2×10^{9}	8.0×10^{9}	5×10^{9}	0.3	0.6
1d	4, 20	4.5×10^{9}	2.1×10^{8}	1.3×10^{10}		24
1d	5, 20	4.5×10^{9}	2.1×10^{8}	7.0×10^{9}	0.3	24
1e	4, 50	7.4×10^{9}	1.7×10^{9}	8.0×10^{9}		2.9
1e	5, 50	7.4×10^{9}	1.7×10^{9}	3.0×10^{9}	0.25	2.9

[a] Conditions: 5% CH_3CN-H_2O, $\mu = 0.5$ ($NaClO_4$). [b] Determined from least-squares fits of the data to eqs 6–8 or 11–13 unless otherwise indicated. Estimated error limits are ±20% for k_r, ±30% for k_s, ±20% for k_{az}'. [c] See text. [d] Assuming $k_{az} = 5 \times 10^9\ M^{-1}\ s^{-1}$. [e] See ref 2b. [f] This rate constant cannot be determined with any accuracy from the fits because it accounts for very little product. The value used here is the approximate diffusion-controlled limit.

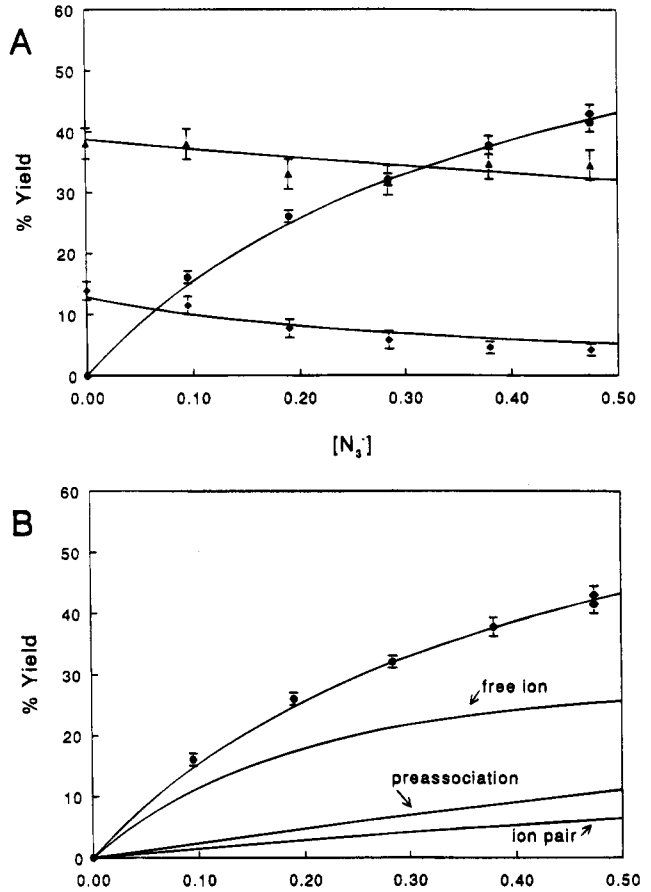

Figure 4. (A) Product yields vs $[N_3^-]$ for **1e** at pH 5.6 in 19/1 N_3^-/HN_3 buffers: (●) **6e** and **20**, Y = Ac, (♦) **4e**, (▲) **8e**. The theoretical curves were calculated from eqs 6–8 for the mechanism of Scheme 4 and the rate constants in Table 2. Nearly identical fits were obtained by fitting the data to eqs 11–13 for the mechanism of Scheme 5. (B) The fit of the N_3^--adduct product yields for **1e** vs $[N_3^-]$ to the preassociation mechanism of Scheme 5. The theoretical curve was calculated from eq 11 and the rate constants in Table 2. The contributions that the free ion, ion pair, and preassociation paths make to the overall N_3^- trapping are indicated.

fits do not indicate that k_s' is significantly different from k_s when the restriction that $k_s = k_s'$ is removed. The values of k_r, $k_s = k_s'$, and k_{az}' which provide the fit to the data shown in Figure 3A are given in Table 2. Significantly poorer fits are obtained if the additional assumption that $k_{az} = k_{az}'$ is made. A fit of the product data for **1e** to the mechanism of Scheme 4 is shown in Figure 4A, and the parameters for the fit are also provided in Table 2.

Both of these esters yield a diazide product **20**, Y = H or Ac, which cannot result from a single one-step substitution reaction. These products can be explained by initial attack of N_3^- at the para-position of **2** or **3** to generate **7d** or **7e**, loss of Cl^- to generate the azido substituted ion **19**, Y = H or Ac, and trapping of this ion by a second N_3^- to generate **20**, Y = H or Ac (Scheme 3). The azido group stabilizes carbenium ions, and azido-substituted carbenium ions are very selective to attack by N_3^- in aqueous solution.[18] If **19**, Y = H or Ac, is similarly selective it will be trapped very efficiently by N_3^- at the $[N_3^-]$ used with **1d** and **1e** (0.0125 M to 0.475 M).

The proportion of the two azide adducts **6** and **20** varies with $[N_3^-]$ for both esters throughout the $[N_3^-]$ range used here. If **6** is considered to be the product of initial ortho-attack and **20** the product of initial para-attack, the ratio of ortho/para attack on the ion pair and free ion can be expressed as

$$(o/p)_{obs} = \left(\frac{1}{1 + f_3/f_2}\right)(o/p)_2 + \left(\frac{f_3/f_2}{1 + f_3/f_2}\right)(o/p)_3 \quad (9)$$

where $f_2 = (1/F)k_{az}'[N_3^-]$, $f_3 = (1/F)(k_{-d}k_{az}[N_3^-]/(k_s + k_{az}[N_3^-]))$, and $(o/p)_2$ and $(o/p)_3$ are the ortho/para product ratios for **2** and **3**, respectively. Equation 9 can be rearranged to eq 10, where the fraction of N_3^- trapping

$$(o/p)_{obs} = (o/p)_3 + f_{ionpair}((o/p)_2 - (o/p)_3) \quad (10)$$

on the ion pair, $f_{ionpair} = 1/(f_3/f_2 + 1)$. This analysis assumes that **7d** and **7e** decompose only by loss of Cl^- to produce **19**, Y = H or Ac. Formation of the ion pairs **18d** and **18e** and their subsequent decomposition into **6d** and **6e** (Scheme 3) was considered unlikely because of the relative leaving group ability of Cl^- and N_3^-[19] and the relative cation-stabilizing effects of Cl and N_3.

Figure 5 shows that there is a linear relationship between $(o/p)_{obs}$ and $f_{ionpair}$ for **1d** and **1e**. For the former compound $(o/p)_3 = 1.30 \pm 0.03$ and $(o/p)_2 = 0.72 \pm 0.13$; for the latter, $(o/p)_3 = 1.08 \pm 0.19$ and $(o/p)_2 = 0.58 \pm 0.20$. In both cases, attack at the ortho position is more favorable in the free ion **3** and attack at the ortho position is more favorable in both **2** and **3** if Y = H. The data indicate that both the counterion in **2** and a bulky Y substituent in **2** and **3** provide steric hindrance to attack at the ortho position.

Previous studies of the reaction of **1e** in the presence of weaker nucleophiles such as Cl^- failed to detect the

(18) Amyes, T. L.; Richard, J. P. *J. Am. Chem. Soc.* **1991**, *113*, 1867–1869.

(19) Amyes, T. L.; Stevens, I. W.; Richard, J. P. *J. Org. Chem.* **1993**, *58*, 6057–6066.

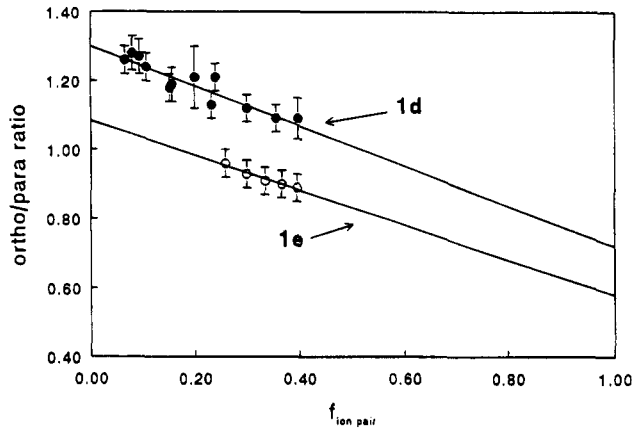

Figure 5. Ortho/para product ratios for the N_3^--adducts derived from **1d** and **1e** vs the fraction of the trapping which occurs through the ion pair, $f_{ionpair}$, assuming the mechanism of Scheme 4. The lines were calculated from a weighted linear least-squares fit of the data.

decrease in the rearrangement product which required the mechanism of Scheme 4.[20] Indeed, the yield of the rearrangement product **9d** only drops from 32 ± 1% to 30 ± 1% as $[Cl^-]$ is increased from 0 to 0.5 M, in hydrolysis reaction mixtures of **1d**. Unless the nucleophile reacts at or very near the diffusion-controlled limit it will not effectively trap **2** at concentrations <1.0 M because this process will not compete with diffusional separation of the ion pair components. According to the rate constants in Table 2, in the absence of N_3^- only 1.4% of **2d** and 8.9% of **2e** are trapped by solvent. In the absence of strong nucleophiles very little of the trapping by both solvent and other added nucleophiles will occur at the ion pair stage for these two compounds.

The best fit rate constant k_{az}' for both **1d** and **1e** shown in Table 2 are somewhat larger than the diffusion-controlled limit. The estimated error limits for these rate constants of ca. ±20% are not large enough to bring them within the range of the approximate diffusion limit for an anion–cation combination reaction in H_2O of ca. 5×10^9 M^{-1} s^{-1}. The magnitudes of k_{az}' are dependent on the choice of k_{-d}, but k_{az}' for **1d** and **1e** could be reduced to the diffusion-controlled limit only by choosing k_{-d} considerably smaller than 10^{10} s^{-1}. This is unlikely to be the case for a diffusion-controlled separation of a cation–anion pair in a predominately aqueous solution.[14] The apparent magnitude of k_{az}' is reduced if a preassociation process (Scheme 5) accounts for some of the N_3^- trapping. A preassociation mechanism can occur only if the ternary complex **23** leads to products faster than it diffuses apart.[4,5] Since N_3^- reacts with the free ions **3g–i**, which are 2 to 4 orders of magnitude less reactive toward solvent than **3d** and **3e**, at diffusion-controlled rates, it is likely that **23d** and **23e** do collapse to product faster than those complexes diffuse apart. The preassociation mechanism will become the predominant pathway for trapping by N_3^- only when **2** reacts with solvent at a rate which precludes diffusional approach of N_3^-. That is not the case for **2d** or **2e**, but the preassociation mechanism can still contribute significantly to the observed N_3^- trapping. The lack of significant change in the hydrolysis rate constant with increasing $[N_3^-]$ for **1d** and **1e** indicates that N_3^- provides no significant assistance to ionization within the diffusional complexes **22d** or **22e** ($k_o \approx k_o'$). Under these conditions the yields of N_3^-- and solvent-derived products, and the rearranged products, are given by eqs 11–13.

$$\%\ \text{azide prods} = \left(\frac{K_{as}[N_3^-]}{1+K_{as}[N_3^-]} + \left(\frac{1}{1+K_{as}[N_3^-]}\right) \times \left(\frac{1}{F}\right)\left(k_{az}'[N_3^-] + \frac{k_{-d}k_{az}[N_3^-]}{k_s + k_{az}[N_3^-]}\right)\right)100 \quad (11)$$

$$\%\ \text{solvent prods} = \left(\frac{1}{1+K_{as}[N_3^-]}\right)\left(\frac{1}{F}\right) \times \left(k_s' + \frac{k_{-d}k_s}{k_s + k_{az}[N_3^-]}\right)100 \quad (12)$$

$$\%\ \text{rearranged} = \left(\frac{1}{1+K_{as}[N_3^-]}\right)\left(\frac{k_r}{F}\right)100 \quad (13)$$

The random association constant K_{as} is assumed to be 0.3 M^{-1} at 20 °C.[4] A value of 0.25 M^{-1} appears to be more appropriate at 50 °C, the temperature at which the data for **1e** were collected (vide infra). The only rate constant that is significantly affected when the preassociation pathway is added to the mechanistic scheme is k_{az}'. To fit the product data to eqs 11–13 the rate constants derived from the fit to eqs 6–8, except k_{az}', were held fixed. In both cases addition of the preassociation pathway reduced k_{az}' to the range expected for a diffusion-controlled rate constant (Table 2) and resulted in fits to the product data which are indistinguishable from those provided by eqs 6–8. Figures 3B and 4B illustrate the contributions that the free ion, the ion pair, and the preassociation mechanism make to the overall N_3^- trapping for **1d** and **1e**. At low $[N_3^-]$, trapping of the free ion accounts for most of the product formation, but the other two paths become more significant at higher $[N_3^-]$. At 0.475 M N_3^-, the free ion, ion pair, and preassociation pathways account for 61%, 22%, and 17%, respectively, of the observed N_3^- trapping for **1d** according to the derived rate constants in Table 2 for the mechanism of Scheme 5. For **1e** the corresponding contributions to the observed trapping are 60%, 15%, and 25%, respectively. Because of the assumptions used in the fitting process, the accuracy of these contributions to the observed trapping cannot be very high, but they do serve to give a reasonable qualitative picture of the relative importance of the three paths for these two esters.

The data shown in Figure 5 do not show any deviations from linearity that would be expected if a third path is contributing to the N_3^- trapping. The relatively large errors in the observed ortho/para product ratios and the shallow dependence of these ratios on $[N_3^-]$ would make it difficult to detect nonlinear behavior unless the ortho/para product ratios for products derived from the ion pair and the preassociation paths are considerably different.

Similar results were obtained for the 4-Me substituted esters **1b** and **1c** (Table 2). For these materials all three paths for N_3^- trapping appear to be significant at $[N_3^-] = 0.1–0.5$ M, and solvent trapping of the ion pair is more significant than in the corresponding 4-Cl substituted esters. The values of k_{az}/k_s for the 4-Cl and 4-Me esters determined from the fits (Table 2) are in reasonable agreement with the observed selectivity ratios S, which are derived from the relative yields of N_3^-- and solvent-

(20) Novak, M.; Pelecanou, M.; Roy, A. K.; Andronico, A. F.; Plourde, F. M.; Olefirowicz, T. M.; Curtin, T. J. *J. Am. Chem. Soc.* **1984**, *106*, 5623–5631.

derived products.[2b] This is due to the fact that most of the N_3^--derived products arise from the free ion and the ion pair which exhibit similar selectivities for N_3^- and solvent.

$S < 1\ M^{-1}$. The trapping situation is very different for the unsubstituted ester **1a**. Trapping by N_3^- is very inefficient. The yields of **6a** and **21**, Y = Ac, amount to only 13% of reaction products at $[N_3^-] = 0.475$ M. This is in the range that can be accounted for entirely by the preassociation pathway. A previously published correlation of log (k_{az}/k_s) vs ΔH of eq 14 calculated by ab initio

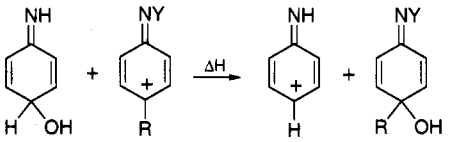

(14)

methods predicted that k_s for **3a** is 1.7×10^{11} s^{-1}.[2b] If this number is used for $k_s = k_s'$, trapping by N_3^- on **2a** or **3a** cannot account for the observed yields of **6a** and **21**, Y = Ac, because k_{az} and k_{az}' are limited by diffusion. Even at $[N_3^-] = 0.5$ M the N_3^- trapping of **2a** or **3a** is less than 2% of solvent trapping. The product data are fit very well by the rate constants of Table 2 (Figure 6). The best fit value of K_{as} of 0.25 M^{-1} is slightly lower than the value of 0.3 M^{-1} usually used at 20 °C.[4] According to this fit, nearly all of the N_3^--derived products are obtained from the preassociation process throughout the $[N_3^-]$ employed in this study. The constant ortho/para product ratio of 0.59 ± 0.01 for **6a/21**, Y = Ac, obtained in 0.1–0.5 M N_3^- is consistent with this conclusion. It is interesting to note that N_3^- shows far less ortho/para selectivity than the solvent (**4a/25** = 0.029 ± 0.003 at $[N_3^-] = 0.0$ to 0.5 M). This is consistent with an N_3^- trapping process which occurs with little or no activation barrier. The less than statistical ortho/para product ratio for **6a/21**, Y = Ac, does indicate some steric hindrance to approach of N_3^- to the ortho positions.

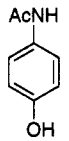

25

The observed N_3^-/solvent selectivity ratio, S, of 0.7 M^{-1} for **1a**[2b] is considerably larger than k_{az}/k_s of ca. 0.03 M^{-1} for **3a** calculated from the fitting procedure. When the preassociation process becomes the major source of the azide adducts it is expected that $S > k_{az}/k_s$. Under these conditions S is governed predominately by the preassociation trapping of **1** by N_3^- which is much more efficient than trapping of **2** or **3** by N_3^- for the highly reactive nitrenium ions that react with solvent with $k_s \geq 10^{10}$ s^{-1}.

Rearrangements and Other Reactions of the Ion Pairs. All of these esters give rise to rearrangement products **8** or **9**, which are assumed (Schemes 1, 4, and 5) to result from internal return, with rearrangement, of the ion pair **2**. The rate constant k_r characterizes this process. Figure 7 shows that k_r does increase with k_s, the rate constant which characterizes the reaction of the free ion and ion pair with solvent. There is an approximately linear relationship between log k_r and log k_s for the esters containing both the SO_4^{2-} and t-$BuCO_2^-$ leaving groups. Figure 7 contains data for all nine esters described in this paper and one other (**1c**, X = C(O)-t-Bu) for which there are sufficient data to make an

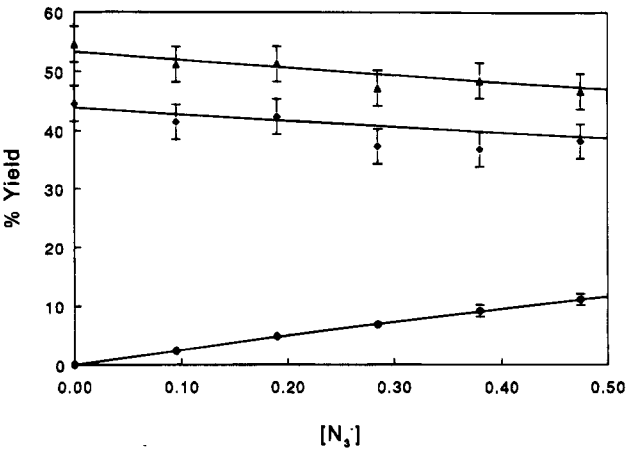

Figure 6. Product yields vs $[N_3^-]$ for **1a** at pH 5.6 in 19/1 N_3^-/HN_3 buffers: (●) **6a** and **21**, Y = Ac, (♦) **4a** and **25**, (▲) **8a**. The theoretical curves were calculated from eqs 11–13 for the mechanism of Scheme 5 and the rate constants in Table 2.

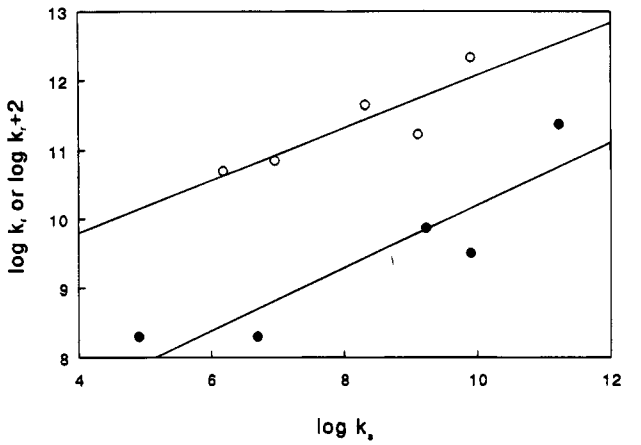

Figure 7. Log k_r vs log k_s for the esters **1**: (●) X = SO_3^-, (○) X = C(O)-t-Bu. The data for **1**, X = C(O)-t-Bu, are displaced vertically by 2.0 units. The lines were calculated from a nonweighted linear least-squares fit of the data.

estimate of k_r based on the k_s value for **3c** reported here.[21] The considerable scatter in Figure 7 is due, in part, to the fact that not all the data were collected at the same temperature and to the accumulated errors introduced by the fitting procedures which assumed single, constant values for k_{-d} and k_{az} throughout the series and which also assumed that $k_s = k_s'$. Errors can also be introduced by small amounts of the rearrangement products which may be present in samples of **1** before the reaction is initiated. This may be particularly important for those esters, such as **1h** and **1i**, which yield very little of the rearrangement products. The slopes of the correlation lines, ca. 0.4–0.5, indicate that the reactions of the anionic leaving groups with the nitrenium ions within the ion pair **2** are less sensitive to electronic effects than are the reactions of H_2O with the same ions.

From the directly measured k_{az} for **3g–i** it is clear that the first-order rate constant for the collapse of N_3^-·**3g–i** > 10^{10} s^{-1}. If this were not the case, k_{az} would not be at or near the diffusion limit for these ions. If the sensitivity of this rate constant to electronic effects is similar to that of k_r for **2** with X = SO_3^- or C(O)-t-Bu, the calculated rate constant for the collapse of N_3^-·**3a** to products exceeds 10^{13} s^{-1}. This indicates that the ion pair is not

(21) Novak, M.; Roy, A. K. *J. Org. Chem.* **1985**, *50*, 4884–4888.

Scheme 6

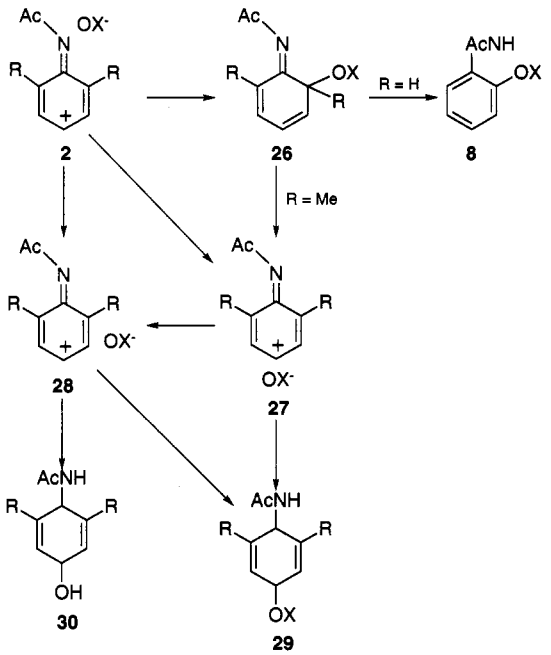

an intermediate in the N_3^- trapping of **3a**. The same conclusion must be made concerning the intermediacy of **23a** in the preassociation trapping of **1a** by N_3^-. This suggests that the preassociation process for **1a** is a concerted reaction. It is not possible to come to a definitive conclusion concerning the intermediacy of **23** in the preassociation trapping by N_3^- of the other esters for which it is observed, but if the first-order rate constant for collapse of N_3^-·**3i** to products is not significantly larger than 10^{10} s^{-1}, **23b–e** would have short, but finite lifetimes.

Variations in product yields with changes in [Br^-] and [H^+] led Fishbein and McClelland to the conclusion that the hydrolysis reactions of *O*-aroyl-*N*-acetyl-*N*-(2,6-dimethylphenyl)hydroxylamines **10** required a mechanism with three intermediates which were identified as ion pairs of different structure.[6] Scheme 6 summarizes their conclusions. The initial ion pair **2** (identical to **2** of Schemes 1, 4, and 5), formed by N–O bond heterolysis, can undergo internal return to produce the cyclohexadiene **26**. In all the cases described in this paper (R = H), **26** can undergo rearomatization to form the rearrangement product **8**. If R = Me this is not possible, and, in the absence of acid catalysis, **26** appears to form another ion pair **27**, which leads to the para-rearrangement product **29**. A third ion pair **28** is required to explain the differences in product yields between **10** and the isolatable **26**.[6] In the reactions of **1a–i** only very small amounts of **29** or products derivable from **29** can be detected (<ca. 5%).[7,20,21] An ion pair such as **27** cannot play a large role in the chemistry of **1a–i**. The 2,6-dimethyl substituents cause a significant difference in the behavior of **1a–i** and **10**. The chemical effect of the methyl groups prevents rearomatization of **26**, and the steric effect of these groups may help to promote structural reorganization of **2**.

It should be pointed out that the mechanisms proposed by Fishbein and McClelland, and ourselves, are not the only ones which can fit these data. Other mechanisms which include three intermediates (or pathways) could also fit the data. We have not attempted to fit our data to Fishbein and McClelland's mechanism because our materials do not produce significant amounts of para-rearrangement products.

Nitrenium Ion Stability and Carcinogenicity. The nitrenium ions **3h** and **3i** have relatively long lifetimes in aqueous solution of ca. 0.2 and 12 μs, respectively.[2,11] These ions react selectively with 2′-deoxyguanosine with rate constants, estimated from experimental $k_{d\text{-}G}/k_s$ ratios, of 1.7×10^9 M^{-1} s^{-1} (**3h**) and 6.2×10^8 M^{-1} s^{-1} (**3i**).[3] The deacetylated ion **3g** behaves similarly, reacting with 2′-deoxyguanosine with an estimated rate constant of 1.8×10^9 M^{-1} s^{-1}.[22] Although these rate constants are somewhat below the diffusion-controlled limit, the reactions of **3g–i** with 2′-deoxyguanosine in aqueous solution are very efficient because their reactions with the solvent are quite slow. These ions are derived from highly carcinogenic sulfuric or carboxylic acid esters,[1] and their high selectivity may be the reason for the high carcinogenicity of *N*-(2-fluorenyl)hydroxylamine and *N*-(4-biphenylyl)hydroxylamine derivatives.

As the nitrenium ions such as **3b–e** become more reactive with solvent, their reactions with nucleophiles such as 2′-deoxyguaosine must become less selective because the second-order rate constants for these reactions (unlike the reaction with solvent) are limited by diffusion to no larger than about 5×10^9 M^{-1} s^{-1}. When $k_s > 10^{10}$ s^{-1}, as with **3a**, no nonsolvent nucleophile can compete with the solvent for the nitrenium ion at moderate nucleophile concentrations. Most trapping by nonsolvent nucleophiles occurs through the inefficient preassociation process. The low efficiency of the trapping reactions of **3a–e** may be related to the low carcinogenic potential of the parent amines and amides.[1]

Experimental Section

The syntheses of the esters **1a–f** and **1i** have been previously described, as have the isolation and characterization of the hydrolysis products of these compounds.[7,8,20,23] General procedures for purification of solvents and other reagents, preparation of solutions for kinetic and product studies, determination of kinetics by UV and HPLC methods, and quantification of reaction products by HPLC have been described.[2,7,8,20,23] Specific procedures used in the N_3^- trapping studies have been published for **1g** and **1h**.[2a] The same procedures were used here. Synthesis of authentic **14**, Y = Ac, and procedures for monitoring its decomposition in aqueous solution have been described.[8]

Analysis of *o*-OSO_3^- rearrangement products such as **8a,c,e,i,i′** by HPLC are complicated by their very short retention times under standard solvent conditions which adequately separate other products. Under these standard conditions these materials elute with the solvent and N_3^-/HN_3 peaks. These products are adequately separated from solvent and N_3^-/HN_3 peaks by ion pair chromatography on the same HPLC column on which the ordinary analyses of other products are performed. The ion pair chromatography is performed by adding 40 mM $(n\text{-Bu})_4N^+HSO_4^-$ to the standard MeOH/H_2O HPLC solvent buffered with 50 mM 1/1 NaOAc/HOAc.

The N_3^- adducts **6a–f,i,i′**, **17f**, **20**, Y = H and Ac, **21**, Y = Ac, and **24** have not been described previously. The isolation and characterization of these materials is described in detail below. The 2-azidoacetanilides were easily identified by the characteristically high frequency chemical shift of the proton ortho to the acetylamino group.[24]

2-Azidoacetanilide (6a) and 4-Azidoacetanilide (21, Y = Ac). A 3 M 19/1 NaN_3/HN_3 buffer was incubated in a water bath at 50 °C for 0.5 h before the addition of 100 mg of **1a** in

(22) Novak, M.; Kennedy, S. A. To be submitted to *J. Am. Chem. Soc.*

(23) Novak, M.; Lagerman, R. K. *J. Org. Chem.* **1988**, *53*, 4762–4769.

(24) Ribera, A.; Rico, M. *Tetrahedron Lett.* **1968**, 535–539. Zanger, M.; Simons, W. W.; Gennaro, A. R. *J. Org. Chem.* **1968**, *33*, 3673–3675.

3 mL of CH_3CN. After 24 h, the solution was extracted with CH_2Cl_2 (3 × 100 mL). The reaction products were separated by TLC on silica gel using 1/1 EtOAc/hexanes as the developing solvent. **6a**: mp 85–86 °C; IR (KBr) 3260, 2135, 2110, 2089, 1683, 1642, 1293, 750 cm^{-1}; ^1H NMR (300 MHz, CD_2Cl_2) δ 8.30–8.27 (1H, m), 7.49 (1H, bs), 7.18–7.09 (3H, m), 2.16 (3H, s); ^{13}C NMR (75.5 MHz, CD_2Cl_2) δ 168.4 (C), 130.0 (C), 128.1 (C), 125.6 (CH), 124.5 (CH), 121.0 (CH), 118.1 (CH), 24.9 (CH_3); high-resolution MS $C_8H_8N_4O$ requires *m/e* 176.0694, found 176.0720. **21**, Y = Ac: mp 117–118.5 °C; IR (KBr) 3313, 2150, 2129, 2117, 1663, 1554, 1262, 831 cm^{-1}; ^1H NMR (200 MHz, $CDCl_3$) δ 7.47 (2H, d, *J* = 8.8 Hz), 7.44 (1H, bs), 6.94 (2H, d, *J* = 8.8 Hz) 2.14 (3H, s); ^{13}C NMR (50.3 MHz, $CDCl_3$) δ 168.4 (C), 135.8 (C), 134.8 (C), 121.4 (CH), 119.4 (CH), 24.3 (CH_3); high-resolution MS $C_8H_8N_4O$ requires *m/e* 176.0694, found 176.0719.

2-Azido-4-methylaniline (6b). To 0.5 mL of 0.5 M N_3^- (19/1 NaN_3/HN_3) in 50/50 D_2O/DMSO-d_6 was injected 24 μL of a 2.5 mM stock of **1b** in DMSO-d_6. The solution was incubated at 20 °C for 30 min before spectra were obtained: ^1H NMR (300 MHz, 50/50 D_2O/DMSO-d_6) δ 6.82 (1H, d, *J* = 1.8 Hz), 6.70 (1H, dd, *J* = 1.8, 4.1 Hz), 6.57 (1H, d, *J* = 4.0 Hz), 1.93 (3H, s); ^{13}C NMR (75.5 MHz, 50/50 D_2O/DMSO-d_6) δ 137.0 (C), 129.6 (C), 127.6 (CH), 126.1 (C), 120.1 (CH), 117.7 (CH), 21.1 (CH_3).

4-Methyl-2-azidoacetanilide (6c). A solution of 163 mg of **1c** in 5 mL of CH_3CN was added to 500 mL of a 2.0 M 19/1 N_3^-/HN_3 buffer at 20 °C. After being stirred overnight, the mixture was extracted (3 × 100 mL) with CH_2Cl_2. The combined extracts were dried over Na_2SO_4, and the solvent was removed by rotary evaporation after filtering. The residue was purified by TLC on silica gel with 4/6 CH_2Cl_2/EtOAc eluent. **6c**: mp 131–133 °C; IR (KBr) 3302, 2116, 1612, 1598, 1234 cm^{-1}; ^1H NMR (300 MHz, CD_2Cl_2), δ 8.13 (1H, d, *J* = 8.0 Hz), 7.40 (1H, s, br), 6.96–6.92 (2H, m), 2.32 (3H, s), 2.12 (3H,s); ^{13}C NMR (75.5 MHz, CD_2Cl_2) δ 168.3 (C), 134.8 (C), 128.1 (C), 127.6 (C), 126.3 (CH), 121.1 (CH), 118.6 (CH), 24.8 (CH_3), 21.0 (CH_3); high-resolution MS $C_9H_{10}N_4O$ requires *m/e* 190.0855, found 190.0853.

The substitution pattern of **6c** was confirmed by its reduction to 2-amino-4-methylacetanilide and comparison to an authentic sample.

2-Amino-4-methylacetanilide. Commercial 4-methyl-2-nitroaniline was acetylated via a standard procedure with acetyl chloride in diethyl ether using *N*-ethylmorpholine as the base. The crude product was recrystallized from ethanol. A 50 mg sample of the acetylated compound was dissolved in 20 mL of glacial acetic acid, 30 mg of 10% Pd/C was added, and the mixture was placed under 50 psi of H_2 overnight. The mixture was filtered through Celite, the solvent was removed by rotary evaporation, and the crude product was purified by column chromatography on silica gel with a solvent gradient from CH_2Cl_2 to 50/50 CH_2Cl_2/EtOAc: mp 130–131.5 °C; ^1H NMR (300 MHz, DMSO-d_6) δ 9.03 (1H, s), 6.98 (1H, d, *J* = 8.0 Hz), 4.75 (2H, s), 6.50 (1H, d, *J* = 1.5 Hz), 6.32 (1H, dd, *J* = 1.5, 8.0 Hz) 2.13 (3H, s), 1.99 (3H, s); ^{13}C NMR (75.5 MHz, DMSO-d_6) δ 168.1 (C), 141.8 (C), 134.7 (C), 125.3 (CH), 121.1 (C), 116.9 (CH), 116.2 (CH), 23.2 (CH_3), 20.8 (CH_3).

Reduction of 6c. This material was reduced in the same manner as described above for 4-methyl-2-nitroacetanilide. NMR spectra of the crude reaction product obtained after removal of the solvent were identical to those of the authentic material.

2-Azido-4-choroaniline (6d) and 2,4-Diazidoaniline (20, Y = H). To 500 mL of 0.5 M 19/1 NaN_3/HN_3 buffer at 0 °C was added 50 mg of **1d** dissolved in 2 mL of CH_3CN. After 24 h, the reaction was extracted three times with CH_2Cl_2. The reaction products were then separated by TLC on silica gel with CH_2Cl_2 as the developing solvent. **6d**: mp 64–65 °C; IR (KBr) 3248, 3323, 2122, 1493, 1276, 848, 650 cm^{-1}; ^1H NMR (200 MHz, $CDCl_3$) δ 6.98 (1H, d, *J* = 2.19 Hz), 6.93 (1H, dd, *J* = 8.46, 2.19 Hz), 6.59 (1H, d, *J* = 8.46 Hz), 3.78 (2H, broad); ^{13}C NMR (75.5 MHz, $CDCl_3$) δ 136.7 (C), 126.1 (C), 125.5 (CH), 123.2 (C), 118.2 (CH), 116.5 (CH); high-resolution MS $C_6H_5N_4$-35Cl requires *m/e* 168.0203, $C_6H_5N_4$37Cl requires *m/e* 170.0173, found 168.0213, 170.0131. **20**, Y = H: 83–85 °C dec; IR (KBr) 3314, 2150, 2129, 2080, 1663, 1507, 1296, 831 cm^{-1}; ^1H NMR (300 MHz, $CDCl_3$) δ 6.65–6.64 (3H, m), 3.75 (2H, bs); ^{13}C NMR (75.5 MHz, $CDCl_3$) δ 135.3 (C), 130.7 (C), 126.3 (C), 116.7 (CH), 116.1 (CH), 109.1 (CH); high-resolution MS $C_6H_5N_7$ requires *m/e* 175.0608, found 175.0624.

4-Chloro-2-azidoacetanilide (6e) and 2,4-Diazidoacetanilide (20, Y = Ac). To 500 mL of 0.5 M, 19/1 NaN_3/HN_3 buffer at 50 °C was added 70 mg of **1e** dissolved in 0.5 mL of CH_3CN. After 29 h, the reaction mixture was extracted (3 × 100 mL) with CH_2Cl_2. After drying over Na_2SO_4 and removal of the solvent, the reaction products were separated by TLC on silica gel with CH_2Cl_2 as the developing solvent. **6e**: mp 149–150 °C; IR (KBr) 3293, 2110, 1666, 1517, 1295, 886 cm^{-1}; ^1H NMR (300 MHz, CD_2Cl_2) δ 8.29 (1H, d, *J* = 8.8 Hz), 7.45 (1H, s), 7.15 (1H, d, *J* = 2.2 Hz), 7.10 (1H, dd, *J* = 2.5, 8.7 Hz), 2.15 (3H, s); ^{13}C NMR (300 MHz, CD_2Cl_2) δ 168.5 (C), 129.4 (C), 129.0 (C), 128.8 (C), 125.7 (CH), 121.9 (CH), 118.2 (CH), 24.9 (CH_3); high-resolution MS $C_8H_7N_4O^{35}Cl$ requires *m/e* 210.0308, $C_8H_7N_4O^{37}Cl$ requires *m/e* 212.0279, found 210.0304, 212.0278. **20**, Y = Ac: mp 133–134 °C; IR (KBr) 3287, 2130, 2120, 1663, 1533, 1262, 836 cm^{-1}; ^1H NMR (300 MHz, CD_2Cl_2) δ 8.31 (1H, d, *J* = 8.8 Hz), 7.43 (1H, s), 6.85 (1H, d, *J* = 2.4 Hz), 6.80 (1H, dd, *J* = 2.3, 9.5 Hz), 2.15 (3H, s); ^{13}C NMR (300 MHz, CD_2Cl_2) δ 168.3 (C), 136.3 (C), 129.8 (C), 127.2 (C) 122.3 (CH), 115.9 (CH), 108.9 (CH), 24.8 (CH_3); high-resolution MS $C_8H_7N_7O$ requires *m/e* 217.0714, found 217.0716.

2-Azido-4-ethoxyacetanilide (6f) and 3-Azido-4-ethoxyacetanilide (17f). To 250 mL of a 0.5 M 1/1 NaN_3/HN_3 solution at 20 °C was added 0.24 mL of a 0.68 M solution of **1f** in CH_3CN. After 12 h, the solution was extracted with CH_2Cl_2 (4 × 50 mL). The resulting mixture of products was separated on a Beckman reversed-phase C18 semi-prep HPLC column with a 1/1 MeOH/H_2O solvent and a flow rate of 3 mL/min. **6f**: mp 108–117 °C; IR (KBr) 3257, 2980, 2925, 2114, 1657, 1298, 836 cm^{-1}; ^1H NMR (300 MHz, $CDCl_3$) δ 8.12 (1H, d, *J* = 9.7 Hz), 7.25 (1H, bs), 6.66–6.62 (2H, m), 4.00 (2H, q, *J* = 6.9 Hz), 2.15 (3H, s), 1.39 (3H, t, *J* = 6.9 Hz); ^{13}C NMR (75.5 MHz, $CDCl_3$) δ 167.9 (C), 155.8 (C), 129.3 (C), 122.7 (C), 122.6 (CH), 110.7 (CH), 104.5 (CH), 63.9 (CH_2), 24.6 (CH_3), 14.7 (CH_3); high-resolution MS $C_{10}H_{12}N_4O_2$ requires *m/e* 220.0962, found 220.0929. **17f**: mp 98–100 °C; IR (KBr) 3254, 3087, 2931, 2112, 1657, 1254, 797 cm^{-1}; ^1H NMR (300 MHz, CD_2Cl_2) δ 7.18 (1H, bs), 7.17 (1H, d, *J* = 2.4 Hz), 7.14 (1H, dd, *J* = 2.4, 8.7 Hz), 6.83 (1H, d, *J* = 8.6 Hz), 4.05 (2H, q, *J* = 6.9 Hz), 2.09 (3H, s), 1.41 (3H, t, *J* = 6.9 Hz); ^{13}C NMR (75.5 MHz, CD_2Cl_2) δ 168.3 (C), 148.7 (C), 132.2 (C), 128.7 (C), 117.5 (CH), 113.7 (CH), 113.3 (CH), 65.5 (CH_2), 24.4 (CH_3), 14.7 (CH_3); high-resolution MS $C_{10}H_{12}N_4O_2$ requires *m/e* 220.0962, found 220.0936.

The ring substitution pattern of **17f** was confirmed by its reduction to 3-amino-4-ethoxyacetanilide which was also synthesized by an independent procedure.

3-Amino-4-ethoxyacetanilide. Step 1. To a small Erlenmeyer flask was added 1 g (5.6 mmol) phenacetin and 1.5 mL of concd H_2SO_4. This mixture was warmed to dissolve the phenacetin and then cooled in an ice bath to 5 °C. A solution of 0.35 mL (5.6 mmol) of concd HNO_3 in 0.56 mL of concd H_2SO_4 was added all at once with stirring. After the resulting mixture was stirred for 2 h at room temperature, 5 mL of water was added. This aqueous mixture was purified by column chromatography on silica gel using EtOAc as the eluent to give a mixture of 4-ethoxy-3-nitroacetanilide[25] and phenacetin: ^1H NMR (300 MHz, $CDCl_3$) δ 8.72 (1H, bs), 7.98 (1H, d, *J* = 2.6 Hz), 7.65 (1H, dd, *J* = 2.6, 9.1 Hz), 6.92 (1H, d, *J* = 9.1 Hz), 4.08 (2H, q, *J* = 6.7 Hz), 2.10 (3H, s), 1.38 (3H, t, *J* = 6.7 Hz). **Step 2.** The recovered mixture was dissolved in 100 mL of EtOAc and placed in a hydrogenation bomb with 30 mg of 10% Pd/C catalyst. This mixture was placed under 50 psi of H_2 for 24 h and filtered. The EtOAc was extracted with 5% HCl. The combined aqueous extracts were adjusted to pH 7 with a solution of NaOH and extracted with EtOAc. The combined organic layers were dried over Na_2SO_4, and the solvent was removed by rotary evaporation. The product was recrystallized from CH_2Cl_2 to give tan crystals: mp 134–136 °C; IR (KBr) 3375, 3285, 3245, 3057, 2974, 2927, 1672, 1560, 1225

(25) Reverdin, F. *Helv. Chim. Acta* **1927**, *10*, 3–4.

cm^{-1}; ^1H NMR (300 MHz, CD_2Cl_2) δ 7.13 (1H, bs), 6.98 (1H, d, J = 2.2 Hz), 6.69 (1H, AB-d, J = 8.6 Hz), 6.64 (1H, AB-dd, J = 2.3, 8.6 Hz), 3.87 (2H, bs), 4.00 (2H, q, J = 7.0 Hz), 2.06 (3H, s), 1.39 (3H, t, J = 6.9 Hz); ^{13}C NMR (75.5 MHz, CD_2Cl_2) δ 168.2, 143.5, 137.2, 132.1, 111.9, 109.6, 107.4, 64.5, 24.5, 15.1.

Reduction of 17f. To a hydrogenation bomb was added 4 mg of **17f** dissolved in ca. 6 mL of EtOAc containing 7.25 mg of 10% Pd/C catalyst. The resulting mixture was placed under 50 psi of H_2 for 4.5 h. The mixture was then filtered and solvent removed by rotary evaporation. The ^1H and ^{13}C NMR spectra of the residue were identical to the authentic 3-amino-4-ethoxyacetanilide.

4-Hydroxy-3-azidoacetanilide (24). To 250 mL of 0.01 M, 1/1 NaN_3/HN_3 buffer at room temperature was added 55 mg of **14**, Y = Ac, dissolved in 2 mL of CH_3CN. After 5 h, the aqueous solution was saturated with NaCl and then extracted three times with EtOAc. The EtOAc extracts were dried over Na_2SO_4 and evaporated to dryness to yield **24** which was 97% pure by HPLC. **24**: mp 117 °C; IR (KBr) 3554, 3483, 3413, 2108, 1619, 1091 cm^{-1}; ^1H NMR (300 MHz, DMSO-d_6) δ 9.78 (s, 1H), 9.77 (s, 1H), 7.29 (d, 1H, J = 2.3 Hz), 7.10 (dd, 1H, J = 2.5, 8.7 Hz), 6.77 (d, 1H, J = 8.7 Hz), 1.97 (s, 1H); ^{13}C NMR (300 MHz, DMSO-d_6) δ 167.9 (C), 145.9 (C), 132.0 (C), 125.2 (C), 116.9 (CH), 116.4 (CH), 111.8 (CH), 23.8 (CH_3); high-resolution MS $C_8H_8N_4O_2$ requires 192.0648, found 192.0648.

1-Azido-*N*-acetyl-2-aminofluorene (6i') and 3-Azido-*N*-acetyl-2-aminofluorene (6i). To 500 mL of a 0.50 M 19/1 NaN_3/HN_3 solution incubated at 20 °C was added with rapid mixing 48.6 mg of **1i** in 2 mL of DMF. After 3 h, the solution was extracted with CH_2Cl_2 (4 × 50 mL). The organic layer was dried over Na_2SO_4. The residue that remained after solvent removal was purified by TLC on silica gel using 9/1 CH_2Cl_2/EtOAc as the developing solvent. **6i'**: mp 161–162.5 °C; IR (KBr) 3281, 2107, 1658, 1537, 1422, 1310 cm^{-1}; ^1H NMR (300 MHz, CD_2Cl_2) δ 8.30 (1H, d, J = 8.4 Hz), 7.75 (1H, d, J = 7.2 Hz), 7.64 (1H, bs), 7.59–7.55 (2H, m), 7.38 (1H, tt, J = 0.6, 7.4 Hz), 7.31 (1H, td, J = 1.3, 7.4 Hz), 4.12 (2H, s), 2.18 (3H, s); ^{13}C NMR (75.5 MHz, CD_2Cl_2) δ 168.4 (C), 142.6 (C), 140.6 (C), 139.4 (C), 135.7 (C), 129.3 (C), 127.4 (CH), 127.1 (CH), 125.2 (CH), 124.9 (C), 120.6 (CH), 120.1 (CH), 117.5 (CH), 34.6 (CH_2), 24.9 (CH_3); high-resolution MS $C_{15}H_{12}N_4O$ requires *m/e* 264.1011, found 264.1010. **6i**: mp 173–174.5 °C; IR (KBr) 3434, 3280, 2124, 1664, 1588, 1420 cm^{-1}; ^1H NMR (300 MHz, CD_2Cl_2) δ 8.53 (1H, s), 7.73 (1H, d, J = 7.3 Hz), 7.59 (1H, bs), 7.54–7.52 (2H, m), 7.37 (1H, td, J = 1.1, 6.3 Hz), 7.29 (1H, td, J = 1.2, 7.4 Hz), 3.89 (2H, s), 2.18 (3H, s); ^{13}C NMR (75.5 MHz, CD_2Cl_2) δ 168.3 (C), 144.2 (C), 141.1 (C), 140.9 (C), 138.0 (C), 128.9 (C), 127.2 (C), 127.1 (CH), 127.0 (CH), 125.4 (CH), 119.7 (CH), 117.5 (CH), 109.3 (CH), 37.3 (CH_2), 25.0 (CH_3); high-resolution MS $C_{15}H_{12}N_4O$ requires *m/e* 264.1011, found 264.1012.

The ring substitution pattern of **6i** was confirmed by its reduction to 3-amino-2-acetamidofluorene which was also prepared by an independent procedure.

3-Amino-2-acetamidofluorene. A 15 mg sample of 3-nitro-2-acetamidofluorene[26] was dissolved in dry THF, and 12 mg of 10% Pd/C was added to the solution. The mixture was placed under 50 psi of H_2 for 4 h and then filtered to remove the catalyst. The product was recovered by evaporation of the solvent: mp 191–192 °C; ^1H NMR (300 MHz, DMSO-d_6) δ 9.13 (1H, s), 7.64 (1H, d, J = 7.4 Hz), 7.49 (1H, d, J = 7.3 Hz), 7.41 (1H, s), 7.32 (1H, t, J = 7.4 Hz), 7.23 (1H, td, J = 1.0, 7.4 Hz), 7.16 (1H, s), 4.89 (2H, s), 3.72 (2H, s), 2.05 (3H, s); ^{13}C NMR (75.5 MHz, DMSO-d_6) δ 168.3, 143.7, 140.9, 141.3, 138.5, 130.8, 126.6, 126.0, 124.9, 123.2, 121.7, 119.1, 106.5, 35.6, 23.4; high-resolution MS $C_{15}H_{14}N_2O$ requires *m/e* 238.1106, found 238.1111.

Reduction of 6i. Five mg of **6i** was dissolved in 6 mL of dry THF, and 8 mg of 10% Pd/C was added to this solution. After 4 h under 50 psi of H_2, the mixture was filtered and the solvent removal by rotary evaporation. ^1H and ^{13}C NMR spectra of the residue were identical to those of authentic 3-amino-2-acetamidofluorene.

Acknowledgment. This work was supported by a grant from the American Cancer Society (CN-23K). Some of the modeling of product data to the reaction schemes was performed by M.N. at the University of New England in Armidale, NSW, Australia. T.G.J. received a NSF-REU Fellowship (CHE-9322137).

Supporting Information Available: Rate constants and product yields of the hydrolysis reactions of **1a–i** in the presence or absence of N_3^-, and ^{13}C NMR spectra for all new N_3^--adducts (20 pages). This material is contained in libraries on microfiche, immediately follows this article in the microfilm version of the journal, and can be ordered from the ACS; see any current masthead page for ordering information.

JO950927V

(26) Bell, F.; Mulholland, D. B. *J. Chem. Soc.* **1949**, 2020–2022.